King's Research Portal

Link to publication record in King's Research Portal

Channel Estimation and Self-Positioning for UAV Swarm

Dian Fan, Feifei Gao, *Senior Member, IEEE*, Bo Ai, , *Senior Member, IEEE*, Gongpu Wang, Zhangdui Zhong, *Senior Member, IEEE*, Yansha Deng, and Arumugam Nallanathan, *Fellow, IEEE*

Abstract—In recent years, unmanned aerial vehicle (UAV) communication technology has played an important role in both military and civilian applications. However, with the rapid development of military equipment, the execution efficiency of single UAVs is often limited, for which complex combat missions cannot be completed well. Therefore, UAV swarm has become an important research trend in the field of UAVs. In this paper, we consider the problem of channel estimation and self-positioning for the UAV swarm, where multiple small UAVs are displaced by arbitrarily unknown displacements due to the dynamic moving. To explore the physical characteristics of UAV swarm, the parameters of the channel are decomposed into the direction of arrival (DOA) information, the relative position information, and the channel gain information. Utilizing the rank reduction (RARE) estimator, DOAs of the different target users can be estimated efficiently, regardless of the position of the UAVs. After obtaining the DOA information, we estimate the channel gain information using small amount of training resources, which significantly reduces the training overhead and the feedback cost. Moreover, the unknown displacements among UAVs can be self-recovered from the mixed integer nonlinear programming (MINLP). To reduce the computational complexity, we develop both the sphere decoding (SD) and the least square (LS) based methods. The deterministic Cramér-Rao bound (CRB) of the self-positioning estimation is derived in closed-form. Finally, numerical examples are provided to corroborate the proposed studies.

Index Terms—Unmanned aerial vehicle (UAV) swarm, DOA estimation, channel estimation, self-positioning.

Dian Fan is with the China Academy of Information and Communications Technology, Beijing 100044, P. R. China (e-mail: fandian@caict.ac.cn). Feifei Gao is with the Department of Automation, Tsinghua University, Beijing 100084, China, also with the Institute for Artificial Intelligence, Tsinghua University, Beijing 100084, China, also with the Beijing National Research Center for Information Science and Technology, Beijing 100084, China, and also with the Key Laboratory of Digital TV System of Guangdong Province and Shenzhen City, Research Institute of Tsinghua University in Shenzhen, Shenzhen 518057, China (e-mail: feifeigao@ieee.org). Bo Ai, and Zhangdui Zhong are with State Key Laboratory of Rail Traffic Control and Safety, Beijing Jiaotong University, Beijing 100044, P. R. China. (e-mail: boai@bjtu.edu.cn, and zhdzhong@bjtu.edu.cn). Gongpu Wang is with School of Computer and Information Technology, Beijing Jiaotong University, Beijing 100044, P. R. China. (e-mail: gpwang@bjtu.edu.cn). Yansha Deng is with Department of Informatics, King's College London, United Kingdom (e-mail: yansha.deng@kcl.ac.uk). Arumugam Nallanathan is with the School of Electronic Engineering and Computer Science, Queen Mary University of London, United Kingdom (e-mail: a.nallanathan@qmul.ac.uk).

I. INTRODUCTION

Due to the cost reduction and device miniaturization, unmanned aerial vehicles (UAVs) have found a wide range of applications such as reconnaissance, surveillance, geodetic survey, emergency assistance etc., and has great application value in military and civilian fields [1], [2]. However, due to the limitations of volume, self-provisioning, flight environment and other factors, complex combat missions cannot be completed well in the single UAV system [3]–[6]. In order to meet the challenges of complex missions and harsh environments, the UAV swarm becomes an important part of UAV cooperation [7]–[10].

UAV swarm is consisted of a number of small UAVs arranged in certain formation to meet the requirements of various missions and tasks, e.g., communicating to the cooperative base stations, users, and detecting the non-cooperative enemy aircraft [11], [12]. UAVs in swarm are small devices equipped with less expensive and less number of antennas, which work in a coordinated manner. Moreover, their ability of handling tasks are also stronger [13], [14]. For example, UAV swarm can jointly perform communications, detection, coverage and other tasks. Moreover, the communications of UAV swarm is robust. The formation of the UAV swarm can be changed due to the dynamically moving, such that the damage to one UAV does not affect the overall performance.

Compared to single UAV system, the key advantages of UAV swarm are summarized here: 1) Only one or two head UAVs may connect to controllers and servers, and then feedback to the other UAVs; 2) UAV swarm is less expensive to acquire, maintain and operate than the single large UAV; 3) Adding more UAVs to the network can easily extend communication umbrella provided by the UAV swarm; 4) The UAV swarm could generally complete the missions more quickly, efficiently and at lower cost.

The performance of the UAV communication systems critically relies on the channel state information (CSI). In general, a large number of UAVs with small antenna array in UAV swarm can constitute a virtual massive multiple input multiple output (MIMO) system, and it can improve spatial resolution, spectrum efficiency, as well as energy efficiency [15]–[18]. Different from the conventional massive MIMO systems, the UAV swarm has the following property: Each UAV is equipped with a fully calibrated small antenna array but the relative position of different UAVs are dynamic, i.e., the positions are generally imprecisely known and vary continuously. Although we can rely on Global Positioning System (GPS) to locate

the position of the UAV, the accuracy provided by GPS can only reach the meter level. Since the displacement among UAVs in the swarm is small or even less than one meter, the accuracy of GPS cannot satisfy the requirement of UAV swarm positioning [19], [20]. In the meantime, UAV swarm would has other missions, such as anti-strike, transportation, search, classification, round-up and so on. At this time, controlling the relative position information of the UAVs is very important.

In this paper, we study the channel estimation and self-positioning problem for UAV swarm. We formulate the channel model, where each UAV is equipped with ideal-calibrated antenna array but the distance among different UAVs are dynamically unknown. To explore the physical characteristics of the channel, we decompose the parameters of each channel into the channel gain, the position and the direction of arrival (DOA) information. We first use a method, called rank reduction (RARE) [21]–[24], to obtain the DOA information of target user blindly. Then we estimate the channel gain information using small amount of training resources, which significantly reduces the training overhead and the feedback cost. Next we propose a self-positioning algorithm to estimate the unknown distances among UAVs. The mathematical approach is shown to fall into the category of mixed integer nonlinear programming (MINLP) and is NP-complete. Nonetheless, we develop two efficient algorithms, i.e., the sphere decoding (SD) and the least square (LS) based methods that greatly reduce the computational complexity compared to the exhaustive searching. We then study the outlier effect, in which spurious UAV positions are misclaimed as the true positions. Several ways to reduce the outlier probability are suggested. Moreover, we derive close form expression for the deterministic Cramér-Rao bound (CRB) to reflect the theoretical lower bound of positioning. Finally, the numerical results are provided to corroborate the proposed studies.

This paper is organized as follows. Section II describes the system model of the proposed UAV swarm. Section III presents the blind DOA estimation and training based channel estimation algorithm of the uplink transmission. Section IV provides the self-positioning algorithm, its related discussions, as well as the derivation of the deterministic CRB. In Section V, we provide various simulation results to evaluate the proposed studies. Finally, conclusions are drawn in Section VI.

Notation: Vectors and matrices are boldface small and capital letters; the transpose, complex conjugate, Hermitian, inverse, and pseudo-inverse of matrix $\mathbf{A}$ are denoted by $\mathbf{A}^T$, $\mathbf{A}^*$, $\mathbf{A}^H$, $\mathbf{A}^{-1}$ and $\mathbf{A}^\dagger$, respectively; $[\mathbf{A}]_{ij}$ denotes the (i,j)th element of $\mathbf{A}$ and $tr(\mathbf{A})$ is the trace of $\mathbf{A}$; $\Re\{\mathbf{A}\}$ and $\Im\{\mathbf{A}\}$ represent the real and the imaginary part of $\mathbf{A}$; $diag\{\mathbf{a}\}$ denotes a diagonal matrix with the diagonal element constructed from $\mathbf{a}$, while $diag\{\mathbf{A}\}$ denotes a vector whose elements are extracted from the diagonal components of $\mathbf{A}$; $\mathbf{I}$ is the identity matrix; $\mathbb{E}\{\cdot\}$ denotes the statistical expectation; $|x|$ is the absolute value of a scalar x; $\lfloor x \rceil$ denotes the nearest integer to x; $\lfloor x \rfloor$ and $\lceil x \rceil$ represent the largest integer that is no bigger than x and the smallest integer that is no less than x, respectively; $\odot$ denotes the Hadamard product.
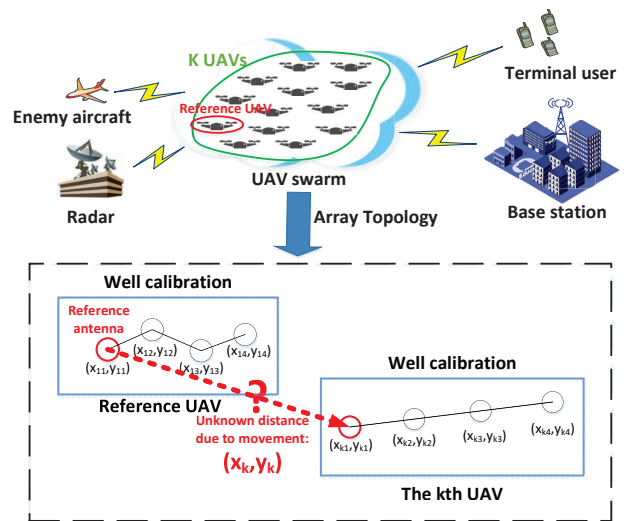

Fig. 1. A typical UAV swarm with various users.

II. System Model

Consider a UAV swarm includes K arbitrary non-overlapping UAVs as shown in Fig. 1, and the kth UAV contains $M_k \geq 1$ antennas. Without loss of generality, we take the first antenna of the first UAV as the reference, and the coordinates of the mth antenna in the kth UAV can be denoted by (x_{km}, y_{km})[1]. We assume that the antennas of each UAV are ideal calibrated but the distances between UAVs are unknown due to the movement of each UAV. In other words, only $x_{km} - x_{kn}$ and $y_{km} - y_{kn}$ for the same k are known a priori. For notation simplicity, we define $x'_{km} \triangleq x_{km} - x_{k1}$ and $y'_{km} \triangleq y_{km} - y_{k1}$ for $m = 2, \cdots, M_k, \forall k$. Clearly, (x'_{km}, y'_{km}) denotes the relative position of the mth antenna in the kth UAV to the first antenna in the same UAV. The communicating partners (called users here) can be the cooperative ground base station, cooperative ground user, large aircraft, air ship, and even the non-cooperative users, i.e. enemy aircraft. Moreover, we assume the signal transmitted by all users are narrowband and mutually uncorrelated.

For UAV communication, UAVs are usually placed at very high altitude such that there are few surrounding scatterers around the UAVs. Actually, only the line of sight (LOS) path contribute to the majority component [16], [25]. Moreover, for UAV swarm, the UAVs are distributed very dense so the relative distance between them is small. Thus, UAV swarm can constitute a virtual massive MIMO system. The uplink channel between the lth user and the UAV swarm can be expressed as

$$\mathbf{h}_l = a_l \mathbf{a}(\theta_l), \tag{1}$$

where $a_l \sim \mathcal{CN}(0,1)$ is the channel gain between the lth user and the UAV swarm, which is independent and identically distributed (i.i.d.). The steering vector $\mathbf{a}(\theta_l)$ of the whole array has the structure, which is shown as (2), where λ is the wave length of the transmitted signals and $\theta_l \in (-90°, 90°)$ is the signal DOA information of the lth user. Then we combine the

---

[1]In order to better describe the algorithm, we tentatively assume that all UAVs are at the same level. But the algorithm can be straightforwardly extend to a more general case.

$$\mathbf{a}(\theta_l) = [1, e^{\frac{j2\pi}{\lambda}(x_{12}\sin\theta_l + y_{12}\cos\theta_l)}, \cdots, e^{\frac{j2\pi}{\lambda}(x_{1M_1}\sin\theta_l + y_{1M_1}\cos\theta_l)},$$

$$\cdots, e^{\frac{j2\pi}{\lambda}(x_{km}\sin\theta_l + y_{km}\cos\theta_l)}, \cdots, e^{\frac{j2\pi}{\lambda}(x_{K1}\sin\theta_l + y_{K1}\cos\theta_l)}, \cdots, e^{\frac{j2\pi}{\lambda}(x_{KM_K}\sin\theta_l + y_{KM_K}\cos\theta_l)}]^T, \quad (2)$$

channel between all users and the UAV swarm into an $M \times L$ channel matrix as

$$\mathbf{H} = [\mathbf{h}_1, \cdots, \mathbf{h}_L] = [a_1\mathbf{a}(\theta_1), \cdots, a_L\mathbf{a}(\theta_L)], \quad (3)$$

where $M = \sum_{k=1}^{K} M_k$ is the total number of antennas of UAV swarm, and L denotes the number of users. Note that the channel matrix $\mathbf{H}$ can be a very large matrix with up to hundreds of rows depending on M. Moreover, the antenna architecture of UAV swarm can achieve high spatial resolution and further improve the channel estimation [26]–[28].

Though formations of the UAV swarm vary from time to time, the rate of formations change is still less than the symbol rate. Hence, we can assume that the formations of the UAV swarm is constant over N symbol intervals, and the received signal can be modeled as

$$\mathbf{x}(t) = \mathbf{Hs}(t) + \mathbf{w}(t)$$
$$= \mathbf{A}(\theta)\mathbf{\Omega s}(t) + \mathbf{w}(t), t = 1, 2, \cdots, N, \quad (4)$$

where $\mathbf{\Omega} = \mathrm{diag}\{a_1, a_2, \cdots, a_L\}$, $\mathbf{A}(\theta) = [\mathbf{a}(\theta_1), \mathbf{a}(\theta_2), \cdots, \mathbf{a}(\theta_L)]$ is the $M \times L$ direction matrix, $\mathbf{s}(t)$ is the $L \times 1$ vector of the signal waveforms from L target users, and $\mathbf{w}(t)$ is the $M \times 1$ vector of noise whose elements are independent random Gaussian variables with the variances σ_n^2. We further decompose $\mathbf{a}(\theta_l)$ as

$$\mathbf{a}(\theta_l) = \mathbf{V}(\theta_l)\mathbf{g}(\theta_l), \quad (5)$$

where

$$\mathbf{V}(\theta_l) = \begin{bmatrix} \mathbf{v}_1(\theta_l) & 0 & \cdots & 0 \\ 0 & \mathbf{v}_2(\theta_l) & \cdots & 0 \\ \vdots & \vdots & \ddots & \vdots \\ 0 & 0 & \cdots & \mathbf{v}_K(\theta_l) \end{bmatrix}, \quad (6)$$

and

$$\mathbf{v}_k(\theta_l) = [1, e^{\frac{j2\pi}{\lambda}(x'_{k2}\sin\theta_l + y'_{k2}\cos\theta_l)},$$
$$\cdots, e^{\frac{j2\pi}{\lambda}(x'_{kM_k}\sin\theta_l + y'_{kM_k}\cos\theta_l)}]^T \quad (7)$$

is the $M_k \times 1$ steering vector of the kth UAV [21], [22]. Moreover,

$$\mathbf{g}(\theta_l) = [1, e^{\frac{j2\pi}{\lambda}(x_{21}\sin\theta_l + y_{21}\cos\theta_l)},$$
$$\cdots, e^{\frac{j2\pi}{\lambda}(x_{K1}\sin\theta_l + y_{K1}\cos\theta_l)}]^T \quad (8)$$

is the $K \times 1$ complex vector associated with the first antenna of each UAV, i.e. $(x_{k1}, y_{k1}), k = 2, 3, \cdots, K$. As seen from (5), $\mathbf{V}(\theta_l)$ characterizes manifold inside each UAV, whereas $\mathbf{g}(\theta_l)$ characterizes unknown positions of all UAVs. From (3) and (5), we know that instead of directly estimating the channel $\mathbf{H}$, one could separately estimate the DOA vector $\theta = [\theta_1, \theta_2, \cdots, \theta_L]^T$, the vector $\mathbf{g}(\theta_l)$, and the corresponding channel gain $a_l, l = 1, 2, \cdots, L$. By doing this, the number

of the parameters to be treated is greatly reduced (from $L \times \sum_{k=1}^{K} M_k$ to $4L-2$). As most array signal processing and communication papers [29]–[33], we assume that the number of users is known for the time being, namely, L is known.

Remark 1. *We will show in the following that if the target user is non-cooperative, the UAV swarm can detect the DOA of the target and can self-locate the relative position among different UAVs. On the other hand, if the target user is a cooperative partner, the UAV swarm can perform channel estimation with the aid of a few pilot symbols.*

III. PARAMETER ESTIMATION

A. RARE Algorithm

DOA aided massive MIMO design has recently attracted significant attention for static and fully calibrated array [26]–[28]. In this subsection, we apply the RARE approach to blindly find the DOA for UAV swarm.

From (4), the covariance matrix of the received signals can be expressed as

$$\mathbf{R} = \mathrm{E}\{\mathbf{x}(t)\mathbf{x}^H(t)\} = \mathbf{A}(\theta)\mathbf{\Omega T\Omega}^H\mathbf{A}^H(\theta) + \sigma^2\mathbf{I}_M, \quad (9)$$

where $\mathbf{T} = \mathrm{E}\{\mathbf{s}(t)\mathbf{s}(t)^H\}$ is the $L \times L$ full-rank covariance matrix of the transmit signal[2], $\sigma^2\mathbf{I}_M = \mathrm{E}\{\mathbf{w}(t)\mathbf{w}(t)^H\}$ is the $M \times M$ full-rank covariance matrix of the noise, and σ^2 is the unknown noise covariance.

The eigen-decomposition of $\mathbf{R}$ can be expressed as

$$\mathbf{R} = \mathbf{U}_s\mathbf{\Lambda}\mathbf{U}_s^H + \sigma^2\mathbf{U}_n\mathbf{U}_n^H, \quad (10)$$

where the $M \times L$ matrix $\mathbf{U}_s$ contains the L signal subspace eigenvectors and the $L \times L$ diagonal matrix $\mathbf{\Lambda}$ contains the corresponding eigenvalues. Similarly, the $M \times (M - L)$ matrix $\mathbf{U}_n$ contains the $M - L$ noise-subspace eigenvectors. Combining (9) and (10) results in

$$\sigma^2\mathbf{U}_n = \mathbf{A}(\theta)\mathbf{\Omega T\Omega}^H\mathbf{A}^H(\theta)\mathbf{U}_n + \sigma^2\mathbf{U}_n. \quad (11)$$

Since the source covariance matrix $\mathbf{T}$ is generally full rank and $\mathbf{A}(\theta)$ is of full column rank, we can obtain

$$\mathbf{a}^H(\theta)\mathbf{U}_n\mathbf{U}_n^H\mathbf{a}(\theta) = 0. \quad (12)$$

Inserting (5) into (12), we can rewrite this equation as

$$\mathbf{a}^H(\theta)\mathbf{U}_n\mathbf{U}_n^H\mathbf{a}(\theta) = \mathbf{g}^H(\theta)\mathbf{V}^H(\theta)\mathbf{U}_n\mathbf{U}_n^H\mathbf{V}(\theta)\mathbf{g}(\theta)$$
$$= \mathbf{g}^H(\theta)\mathbf{C}(\theta)\mathbf{g}(\theta) = 0, \quad (13)$$

where the $K \times K$ matrix $\mathbf{C}(\theta) = \mathbf{V}^H(\theta)\mathbf{U}_n\mathbf{U}_n^H\mathbf{V}(\theta)$ is defined as the *determination matrix*.

---

[2]Assuming that the LTE system has a bandwidth of $20M$ and 10 users, transmitting 10 symbols are actually only need 0.5 milliseconds. During this period, the moving distance of UAV is only $4cm$ when the moving velocity of the UAV is 80km/h. Therefore, the DOA can be assumed unchanged in the far field UAV swarm.

We can easily observe from (13) that the coordinate parameter is contained in $\mathbf{g}(\theta)$ only, so that the matrix $\mathbf{C}(\theta)$ is independent of the coordinate parameter of different UAVs. Bearing in mind that the column rank of $\mathbf{U}_n$ is $M - L$, if $K \leq M - L$, which is usually the case when $M_k \geq 2$ for each UAV, then $\mathbf{C}(\theta)$ is full rank. Therefore, (13) tells that the matrix $\mathbf{C}(\theta)$ drops rank at each DOA, and DOAs from different users can be found from the following equation

$$\det\{\mathbf{C}(\theta)\} = 0. \tag{14}$$

Remark 2. *Define* $b_k = 0$ *when the antenna displacement of the kth UAV is greater than $\lambda/2$; otherwise $b_k = 1$. To ensure RARE estimator works, it must satisfy $\sum_{k=1}^{K} b_k(M_k - 1) \geq L, b_k = 0, 1$, namely, the total number of antennas in the UAV swarm minus the number of UAV is greater than or equal to the number of target users. If the number of target users is large while the number of antennas in each UAV is small, i.e. $M_k \leq L$, for $k = 1, 2, \cdots, K$, each UAV cannot individually detect L target users. Nevertheless, the teamwork from UAV swarm could still detect all L target.*

B. Estimating $\mathbf{g}(\theta)$

It is seen from (13) that $\mathbf{g}(\theta_l)$ stays in the null space of $\mathbf{C}(\theta)$. To guarantee the uniqueness of $\mathbf{g}(\theta_l)$, we need to make sure that $\mathbf{g}(\theta_l)$ has only one zero eigenvalue in the noiseless scenario. Let us provide the following theorem:

Theorem 1. *If $\sum_{k=1}^{K} b_k(M_k - 1) \geq L$ holds, then matrix $\mathbf{C}(\theta)$ has a unique zero eigenvalue for each $\theta_l, l = 1, 2, \cdots, L$.*

Proof: From (13), we know that the following equations hold only for the true DOAs $\theta_l, l = 1, 2, \cdots, L$:

$$\mathbf{g}^H(\theta_l)\mathbf{C}(\theta_l)\mathbf{g}(\theta_l) = 0. \tag{15}$$

Consequently, $\mathbf{C}(\theta_l)$ drops rank and has at least one zero eigenvalue. An equivalent expression of (15) is written as

$$\mathbf{U}_n^H \mathbf{V}(\theta_l)\mathbf{g}(\theta_l) = \mathbf{U}_n^H \mathbf{a}(\theta_l) = \mathbf{0}, \tag{16}$$

which says that the steering vector $\mathbf{a}(\theta_l)$ lies in the signal-subspace spanned by $\mathbf{U}_s$.

Lemma 1. *Let*

$$\tilde{\mathbf{a}}(\theta) = \mathbf{V}(\theta)\boldsymbol{\gamma} = \sum_{i=1}^{K} \gamma_i \tilde{\mathbf{v}}_i(\theta) \tag{17}$$

be the linear combination of K element-orthogonal vectors $\tilde{\mathbf{v}}_i(\theta)$, where $\tilde{\mathbf{v}}_i(\theta)$ is the ith column of matrix $\mathbf{V}(\theta)$, and $\boldsymbol{\gamma} = [\gamma_1, \gamma_2, \cdots, \gamma_K]^T$ is an arbitrary $K \times 1$ complex vector. Define $\tilde{\mathcal{M}} = \{\tilde{\mathbf{a}}(\theta) : \theta \in \Theta\}$ as the set of all $\tilde{\mathbf{a}}(\theta)$, $\Theta \in [-\frac{\pi}{2}, \frac{\pi}{2}]$. Using the property that $\tilde{\mathbf{v}}_i(\theta)$ is element-orthogonal and that $\tilde{\mathbf{v}}_i(\theta)$ is the steering vector of the ith UAV, one can conclude that any $\sum_{k=1}^{K} b_k(M_k - 1)$ vectors taking nonidentical values of θ from set $\tilde{\mathcal{M}}$ are linearly independent [22].

Suppose $\mathbf{C}(\theta_1)$ has more than one zero eigenvalues. Then, there exists a vector γ that is linearly independent from $\mathbf{h}(\theta_1)$ and satisfies

$$\boldsymbol{\gamma}^H \mathbf{C}(\theta_1)\boldsymbol{\gamma} = 0. \tag{18}$$

Equivalently, we have

$$\mathbf{U}_n \mathbf{V}(\theta_1)\boldsymbol{\gamma} = \mathbf{0}. \tag{19}$$

Therefore, $\mathbf{V}(\theta_1)\boldsymbol{\gamma}$ also stays in the signal-subspace. In addition, it is not difficult to know that $\mathbf{V}(\theta_1)\boldsymbol{\gamma}$ and $\mathbf{V}(\theta_1)\mathbf{g}(\theta_1)$ are linearly independent.

Since the signal space is spanned exactly by the L steering vectors $\mathbf{V}(\theta_1)\mathbf{g}(\theta_1), \mathbf{V}(\theta_1)\boldsymbol{\gamma}$ could be written as the linear combination of these L steering vectors, namely

$$\mathbf{V}(\theta_1)\boldsymbol{\gamma} = \alpha_1 \mathbf{V}(\theta_1)\mathbf{g}(\theta_1) + \alpha_2 \mathbf{V}(\theta_2)\mathbf{g}(\theta_2) + \cdots + \alpha_L \mathbf{V}(\theta_L)\mathbf{g}(\theta_L), \tag{20}$$

for $[\alpha_1, \alpha_2, \cdots, \alpha_L]^T \neq \mathbf{0}$. The above equation can be rewritten as

$$\mathbf{V}(\theta_1)(\boldsymbol{\gamma} - \alpha_1 \mathbf{g}(\theta_1)) = \alpha_2 \mathbf{V}(\theta_2)\mathbf{g}(\theta_2) + \cdots + \alpha_L \mathbf{V}(\theta_L)\mathbf{g}(\theta_L). \tag{21}$$

From the independence between $\boldsymbol{\gamma}$ and $\mathbf{g}(\theta_1)$, we know $(\boldsymbol{\gamma} - \alpha_1 \mathbf{g}(\theta_1)) \neq \mathbf{0}$ for any α_1. Therefore, (21) indicates the linear dependence among $\mathbf{V}(\theta_1)(\boldsymbol{\gamma} - \alpha_1 \mathbf{g}(\theta_1))$ and $\mathbf{V}(\theta_i)\mathbf{g}(\theta_i), i = 2, 3, \cdots, L$, which forms clear contradiction with Lemma 1. As a result, we draw the conclusion that $\mathbf{C}(\theta_1)$ cannot have more than one zero eigenvalues. Similar discussion applies to all other $\mathbf{C}(\theta_l)$ and Theorem 1 is proved. ∎

From Theorem 1, we know that a unique null-space eigenvector of $\mathbf{C}(\theta_1)$, denoted as $\mathbf{u}_l$ is co-linear with $\mathbf{g}(\theta_1)$ can be found for each θ_l. Since the first element of $\mathbf{g}(\theta_l)$ is always 1, we can obtain $\mathbf{g}(\theta_l)$ from

$$\hat{\mathbf{g}}(\theta_l) = \mathbf{u}_l / u_{l,1}, \tag{22}$$

where $u_{l,1}$ is the first element of $\mathbf{u}_l$.

Remark 3. *Practically when there are only a finite number of data samples, the covariance matrix is replaced with the sample covariance matrix and $\mathbf{u}_l$ is found from the eigenvector of $\mathbf{C}(\theta_1)$ that corresponds to the smallest eigenvalue.*

C. Training based Channel Gain Estimation Algorithm

For cooperative users, we can further calculate channel gain to recover the overall channel $\mathbf{h}$. We assume there are $P = L$ orthogonal training sequences with length L. Then each user sends the orthogonal training sequence to obtain their channel estimate in the uplink stage. Denote the available orthogonal training sequences set as $\mathbf{S} = [\mathbf{s}_1, \mathbf{s}_2, \cdots, \mathbf{s}_L]$, with $\mathbf{s}_i^H \mathbf{s}_j = P \cdot \sigma_p^2 \cdot \delta(i - j)$ and σ_p^2 being the average training power. The received training signals $\mathbf{Y}$ at the UAV swarm can be written as

$$\mathbf{Y} = \mathbf{H}\mathbf{S}^H + \mathbf{N} = \sum_{l=1}^{L} a_l \mathbf{a}(\theta_l)\mathbf{s}_l^H + \mathbf{N}$$
$$= \sum_{l=1}^{L} a_l \mathbf{V}(\theta_l)\mathbf{g}(\theta_l)\mathbf{s}_l^H + \mathbf{N}, \tag{23}$$

where $\mathbf{N}$ is the independent additive white Gaussian noise matrix with elements distributed as $\mathcal{CN}(0, 1)$. Hence, the

estimation of the channel gain a_l can be expressed as

$$
\begin{aligned}
\hat{a}_l &= \frac{1}{P\sigma_p^2} \cdot \frac{(\mathbf{V}(\theta_l)\mathbf{g}(\theta_l))^H}{\|\mathbf{V}(\theta_l)\mathbf{g}(\theta_l)\|^2}\mathbf{Y}\mathbf{s}_l \\
&= \frac{1}{P\sigma_p^2} \cdot \frac{(\mathbf{V}(\theta_l)\mathbf{g}(\theta_l))^H}{\|\mathbf{V}(\theta_l)\mathbf{g}(\theta_l)\|^2}\left(\sum_{l=1}^{L} a_l\mathbf{V}(\theta_l)\mathbf{g}(\theta_l)\mathbf{s}_l^H + \mathbf{N}\right)\mathbf{s}_l \\
&= a_l + \frac{1}{P\sigma_p^2} \cdot \frac{(\mathbf{V}(\theta_l)\mathbf{g}(\theta_l))^H}{\|\mathbf{V}(\theta_l)\mathbf{g}(\theta_l)\|^2}\mathbf{N}\mathbf{s}_l \\
&= a_l + \frac{1}{\sqrt{P\frac{\sigma_p^2}{\sigma_n^2}}} \cdot \frac{(\mathbf{V}(\theta_l)\mathbf{g}(\theta_l))^H}{\|\mathbf{V}(\theta_l)\mathbf{g}(\theta_l)\|^2}\mathbf{N},
\end{aligned} \tag{24}
$$

where $\frac{\sigma_p^2}{\sigma_n^2}$ is defined as the uplink training signal-to-noise ratio (SNR).

Repeating the similar operations in (24) yields the channel gain estimates for all users. With the DOA information from RARE algorithm (14), positioning information from (22), and channel gain information from (24), we may obtain the uplink channel estimation for all users as

$$
\hat{\mathbf{h}}_l = \hat{a}_l\hat{\mathbf{V}}(\theta_l)\hat{\mathbf{g}}(\theta_l). \tag{25}
$$

IV. UAV SELF-POSITIONING

Since the array in each UAV is ideally calibrated, it suffices to find the position of the first antenna of each UAV, i.e., $\{(x_{k1}, y_{k1})\}_{k=2}^K$, which are contained in the vector $\mathbf{g}(\theta_l), l = 1, 2, \cdots, L$. The target now is to estimate $(x_{k1}, y_{k1})_{k=2}^K$ from the kth entry of $\mathbf{g}(\theta_l), l = 1, 2, \cdots, L$. Due to symmetry, we only need to discuss for $k = 2$. The following L equations could be obtained:

$$
\frac{2\pi}{\lambda}(x_{21}\sin\theta_l + y_{21}\cos\theta_l) - 2\pi n_l = \angle g_2(\theta_l), \tag{26}
$$

where $\angle g_2(\theta_l) \in [-\pi, \pi)$ is the phase of $g_2(\theta_l)$ and $2\pi n_l$ (n_l can be any integer) is the phase delay ambiguity (PDA). For notation simplicity, we normalize (x_{21}, y_{21}) by λ and define

$$
x = x_{21}/\lambda, \quad y = y_{21}/\lambda, \quad \angle g_2(\theta_l)/2\pi = c_l. \tag{27}
$$

Equation (26) could be reformulated as

$$
x\sin\theta_l + y\cos\theta_l - n_l = c_l, l = 1, 2, \cdots, L. \tag{28}
$$

Since the range of c_l is $[-0.5, 0.5]$, the integer ambiguity in PDA can be bounded in

$$
|n_l| \leq |x\sin\theta_l + y\cos\theta_l + 0.5| \leq \sqrt{x^2 + y^2} + 0.5 \\
= \lfloor\sqrt{x^2 + y^2}\rceil. \tag{29}
$$

Clearly, PDA is a non-preferred phenomenon that gives wrong estimation over antenna positions. Although PDA is inherent for each equation in (28), with multiple equations $L \geq 1$ it is possible to eliminate the PDAs for every equation.

A. Necessary and Sufficient Condition (NASC) for No PDA

Denote d as the maximum possible radius (normalized by λ) of the area in which the UAV resides. Define

$$
\mathbf{G} = \begin{bmatrix} \sin\theta_1 & \cos\theta_1 \\ \sin\theta_2 & \cos\theta_2 \\ \vdots & \vdots \\ \sin\theta_L & \cos\theta_L \end{bmatrix}, \mathbf{n} = \begin{bmatrix} n_1 \\ n_2 \\ \vdots \\ n_L \end{bmatrix}, \mathbf{\Delta n} = \begin{bmatrix} \Delta n_1 \\ \Delta n_2 \\ \vdots \\ \Delta n_L \end{bmatrix}. \tag{30}
$$

An NASC for no PDA has been derived in [23], and is modified here for our considered system model:

Lemma 2. *The NASC for non-existence of PDA from equation (28) can be expressed as*

$$
rank\{[\mathbf{G}, \Delta\mathbf{n}]\} = 3, \tag{31}
$$

for

$$
\Delta\mathbf{n} \neq \mathbf{0}, \quad |n_l + \Delta n_l| \leq \lfloor d \rfloor, \quad n_l \leq \lfloor d \rfloor. \tag{32}
$$

The last two terms in (32) *could be equivalently expressed as* $\Delta n_l \in \tilde{\mathcal{L}} \triangleq \{-2\lfloor d\rfloor, -2\lfloor d\rfloor + 1, \cdots, 2\lfloor d\rfloor - 1, 2\lfloor d\rfloor\}$.

Obviously, there is no PDA if $d < \frac{1}{2}$, where all n_l's have to be 0. In this case, (x, y) could be obtained as long as $L \geq 2$. However, for more general radius where d is greater than $\frac{1}{2}$, $L \geq 3$ is normally required in order to estimate (x, y) from (28) without encountering PDA.

From matrix theory, it is equivalent to check whether following inequality holds

$$
\det\left\{\begin{bmatrix} \sin\theta_{l1} & \cos\theta_{l1} & \Delta n_{l1} \\ \sin\theta_{l2} & \cos\theta_{l2} & \Delta n_{l2} \\ \sin\theta_{l3} & \cos\theta_{l3} & \Delta n_{l3} \end{bmatrix}\right\} \neq 0, \tag{33}
$$

for one pair of (l_1, l_2, l_3) with $l_i \in \{1, 2, \cdots, L\}$.

Theorem 2. *When the DOAs are randomly drawn from* $[-\frac{\pi}{2}, \frac{\pi}{2})$, *the probability for* (33) *to hold is 1.*

Proof: Instead of proving (33), we would rather prove that the probability of

$$
\det\left\{\begin{bmatrix} \sin\theta_1 & \cos\theta_1 & \Delta n_1 \\ \sin\theta_2 & \cos\theta_2 & \Delta n_2 \\ \sin\theta_3 & \cos\theta_3 & \Delta n_3 \end{bmatrix}\right\} = 0 \tag{34}
$$

is zero for

$$
[\Delta n_1, \Delta n_2, \Delta n_3] \neq \mathbf{0}, \quad \text{and} |\Delta n_l| \in \tilde{\mathcal{L}}. \tag{35}
$$

The following equality could be obtain from (34):

$$
\Delta n_1\sin(\theta_2 - \theta_3) + \Delta n_2\sin(\theta_3 - \theta_1) \\
+ \Delta n_3\sin(\theta_1 - \theta_2) = 0. \tag{36}
$$

Let $\alpha = \theta_2 - \theta_3$, $\beta = \theta_3 - \theta_1$ and define $\varphi = \arctan\frac{\Delta n_3\sin\beta}{\Delta n_1 - \Delta n_3\cos\beta}$. The equation (36) is converted into

$$
\sin(\alpha - \varphi) = -\frac{\Delta n_2\sin\beta}{\sqrt{\Delta n_1^2 - 2\Delta n_1\Delta n_3\cos\beta + \Delta n_3^2}}. \tag{37}
$$

If β is fixed, the equation (37) holds for at most $(4\lfloor d\rfloor + 1)^3$ different α, each corresponding to a different combinations of Δn_1, Δn_2, and Δn_3. Therefore, conditioned on fixed θ_3 and

θ_1, there exist no more than $(4\lfloor d \rfloor + 1)^3$ different θ_2 that satisfy (34). Let us divide $[-\frac{\pi}{2}, \frac{\pi}{2}]$ to m intervals with $m \to \infty$. The probability of (34) satisfies

$$P\{(34)\} \leq \lim_{m \to \infty} \frac{C_m^2 \times (4\lfloor d \rfloor + 1)^3}{C_m^3} = 0. \qquad (38)$$

The Lemma have been proved. ∎

Since it is not convenient to work with the rank of a matrix, an alternative NASC for no PDA is expressed as

$$\mathbf{P}_{\boldsymbol{\theta}}^{\perp} \Delta \mathbf{n} \neq \mathbf{0}, \qquad (39)$$

for

$$\Delta \mathbf{n} \neq \mathbf{0}, \quad \text{and} \quad \Delta n_l \in \tilde{\mathcal{L}}, \qquad (40)$$

where $\mathbf{P}_{\boldsymbol{\theta}}^{\perp} = \mathbf{I} - \mathbf{P}_{\boldsymbol{\theta}}$ and $\mathbf{P}_{\boldsymbol{\theta}}$ denotes the projection matrix onto the subspace spanned by $\mathbf{G}$. From the Appendix, $\mathbf{P}_{\boldsymbol{\theta}}$ could be simply calculated from

$$\mathbf{P}_{\boldsymbol{\theta}} = \frac{1}{D} \mathbf{B} \mathbf{B}^T, \qquad (41)$$

where

$$D = \sum_i \sum_{j > i} \sin^2(\theta_i - \theta_j), \qquad (42)$$

$$[\mathbf{B}]_{ij} = \sin(\theta_j - \theta_i). \qquad (43)$$

<u>Remark</u> 4. *Condition* (39) *is easier to be checked in practice when the received signals are corrupted by the noise. In this case, those Δn_l's, which make* (31) *full rank but satisfy*

$$\mathbf{P}_{\boldsymbol{\theta}}^{\perp} \Delta \mathbf{n} \approx \mathbf{0}, \qquad (44)$$

may still be subject to PDA.

B. Practical Algorithms for UAV Self-positioning

The goal is to find two real unknowns x, y, and L integers $\{n_l\}_{l=1}^L$ from L equations (28). The problem is classified into the so called mixed integer linear equations (MINLE) [38], which describes the generalization of the linear systems [39] and the diophantine systems [40]. However, in the noisy case all the equalities in (28) only hold approximately. As a result, the pure mathematical approach provided in [38] cannot be applied directly. We then propose to estimate the variables by minimizing the difference between the left-hand side (LHS) and right-hand side (RHS) of (28).

Define

$$\mathbf{c} = [c_1, c_2, \cdots, c_L]^T, \quad \mathbf{b} = \mathbf{c} + \mathbf{n}, \quad \mathbf{z} = [x, y]^T. \qquad (45)$$

The following constrained optimization criterion is obtained:

$$\min_{x, y, \mathbf{n}} \quad \epsilon \triangleq \|\mathbf{G}\mathbf{z} - \mathbf{b}\|^2 \qquad (46)$$
$$\text{s. t.} \quad x^2 + y^2 \leq d^2,$$
$$n_l \in \mathcal{L} \triangleq \{-\lfloor d \rfloor, -\lfloor d \rfloor + 1, \cdots, \lfloor d \rfloor - 1, \lfloor d \rfloor\}.$$

In fact, ϵ is the least square error (LSE) that unbalances the equalities (28). Optimization in (46) falls into the category of the so called mixed integer nonlinear programming (MINLP) [41] which is generally hard to solve. In this paper, we propose two efficient algorithms to solve (46) by utilizing the special structure of (28).

1) Constrained Sphere Decoding (SD) Approach: From (28), the LS solution of $\mathbf{z}$ is expressed as

$$\mathbf{z} = \mathbf{G}^{\dagger} \mathbf{b}. \qquad (47)$$

Substituting (47) into (46) gives the new optimization over the integers $\mathbf{n}$ as

$$\min_{\{n_l\}_{l=1}^L} \quad \|\mathbf{P}_{\boldsymbol{\theta}}^{\perp}(\mathbf{n} + \mathbf{c})\|^2 \qquad (48)$$
$$\text{s. t.} \quad \|\mathbf{G}^{\dagger}\mathbf{b}\|^2 \leq d^2,$$
$$n_l \in \mathcal{L}, \quad l = 1, 2, \cdots, L.$$

Since the values of n_l are integers in $\mathcal{L}$, the problem is equivalent to finding the closest lattice point from the center $-\mathbf{P}_{\boldsymbol{\theta}}^{\perp}\mathbf{c}$. Instead of the naive searching, the sphere decoding SD algorithm [29], [30] could be applied to find the solution with expected complexity $O(L^{e_c})$, where e_c is some constant related with SNRs, the size of the lattice, and the number of DOAs. The SD algorithm has been intensively discussed in the literature [29], [30] and the references therein, while the details will be omitted in this paper. Yet, several special attentions that should be paid to (48) are provided here:

1) Not like [29], where the initial radius C_0 could be selected from chi-square distribution according to the predetermined probability, the selection of C_0 in (48) is more complicated. This is mainly due to that the statistics of the perturbation in the estimated θ_l and c_l are difficult to characterize. Hence, one may randomly choose a valid $\mathbf{n}_0$ and set $C_0 = \|\mathbf{P}_{\boldsymbol{\theta}}^{\perp}(\mathbf{n}_t + \mathbf{c})\|^2$. A more sophisticated way may require some off-line efforts to numerically obtain the statistics of $\|\mathbf{P}_{\boldsymbol{\theta}}^{\perp}(\mathbf{n}_t + \mathbf{c})\|^2$.

2) The matrix $\mathbf{P}_{\boldsymbol{\theta}}^{\perp}$ drops rank by 2. In this case, the generalized SD could be applied [31], where the SD is in fact applied to $n_3, \cdots, n_N$ for each possible deterministic pair n_1, n_2. The complexity is proportional to $(2\lfloor d \rfloor + 1)^2 O((L-2)^{e_c})$ regardless of the SNR.

3) The valid lattice point should not only stay in an intermediate radius but also satisfy the additional constraint $\|\mathbf{G}^{\dagger}\mathbf{b}\|^2 \leq d^2$. Since $\mathbf{G}^{\dagger}$ only needs to be calculated once, the related complexity can be ignored. Therefore, around $(4L+1)$ additional flops are needed once a lattice point is found in the intermediate radius.

2) LS Based Approach: The complexity of the SD algorithm is still high if the initial radius C_0 is large. We then develop an LS estimation algorithm which requires only linear complexity. If we specify the values of n_1 and n_2, we can rewrite (28) as:

$$\underbrace{\begin{bmatrix} \sin \theta_1 & \cos \theta_1 & 0 & \cdots & 0 \\ \sin \theta_2 & \cos \theta_2 & 0 & \cdots & 0 \\ \sin \theta_3 & \cos \theta_3 & 1 & \cdots & 0 \\ \vdots & \vdots & 0 & \ddots & 0 \\ \sin \theta_L & \cos \theta_L & 0 & \cdots & 1 \end{bmatrix}}_{\boldsymbol{\Lambda}} \underbrace{\begin{bmatrix} x \\ y \\ n_3 \\ \vdots \\ n_L \end{bmatrix}}_{\boldsymbol{\nu}} = \mathbf{c} + \underbrace{\begin{bmatrix} n_1 \\ n_2 \\ 0 \\ \vdots \\ 0 \end{bmatrix}}_{\boldsymbol{\eta}},$$

$$(49)$$

where $\boldsymbol{\Lambda}, \boldsymbol{\nu}$, and $\boldsymbol{\eta}$ are defined as the corresponding items. Obviously, $\boldsymbol{\Lambda}$ is non-singular, so $\boldsymbol{\nu}$ can be uniquely determined

by multiplying $\boldsymbol{\Lambda}^{-1}$ to both sides of (49). Note that $\boldsymbol{\Lambda}^{-1}$ only needs to be calculated once, while for different choices of (n_1, n_2) only $\boldsymbol{\Lambda}^{-1}\boldsymbol{\eta}$ is re-calculated. Therefore, the number of flops for calculating each $\boldsymbol{\nu}$ is approximated by $3L$. Based on the values of the last $L-2$ entries of $\boldsymbol{\nu}$, we would determine whether the current pair (n_1, n_2) is valid or not. Specifically, we first set a threshold τ. If there exists an l_0 with $3 \le l_0 \le L$ such that $|\nu_{l_0} - \lfloor \nu_{l_0} \rceil| > \tau$, then the current pair (n_1, n_2) should be discarded. Furthermore, if any of $\lfloor \nu_{l_0} \rceil$ stays outside $\mathcal{L}$, the current of (n_1, n_2) should be discarded. After a group of valid integers $\{n_l\}_{l=1}^L$ is found, an LS estimate of (x, y) can be obtained from (47) with $5L-2$ flops. We need to check whether the obtained (x, y) stays in the presumed region and the false candidates should also be discarded, which requires 3 flops. All the candidates (x, y) and their corresponding $\mathbf{n}$ are then substituted back to (46) to obtain LSE ϵ. The number of flops for this step is around $6L - 1$. Finally, the group of $\{x, y, \mathbf{n}\}$ that gives the minimum LSE will be selected. From all the above, the overall complexity to find the optimal solution is upper bounded by $14L(2\lfloor d \rfloor + 1)^2$ in the worst case. Based on the discussion so far, the proposed LS-based positioning can be summarized in **Algorithm** 1.

Algorithm 1 LS-based positioning algorithm

Input: Covariance matrix: $\mathbf{R}$; Maximum radius: d; Threshold: τ.
Output: Estimated DOAs $\{\theta_l\}_{l=1}^L$ for all users, and estimated positioning $\{(x_{k1}, y_{k1})\}_{k=2}^K$.
Initialization: LSE $\epsilon = 999$.
1.   Obtain the noise-subspace matrix $\mathbf{U}_n$ from the eigen-decomposition of $\mathbf{R}$.
2.   Calculate the DOAs $\{\theta_l\}_{l=1}^L$ for all users from (14), where $\mathbf{C}(\theta_l) = \mathbf{V}^H(\theta_l))\mathbf{U}_n\mathbf{U}_n^H\mathbf{V}(\theta_l)$.
3.   Calculate the non-space eigenvector $\mathbf{u}_l$ of $\mathbf{C}(\theta_l)$ and obtain $\mathbf{g}(\theta_l)$ from (22) for any $l = 1, 2, \cdots, L$.
4.   Calculate the set of integer ambiguity $\mathcal{L} = \{-\lfloor d \rfloor, -\lfloor d \rfloor + 1, \cdots, \lfloor d \rfloor - 1, \lfloor d \rfloor\}$.
5.   **For** $n_1 \in \mathcal{L}$, $n_2 \in \mathcal{L}$
6.   Calculate $\boldsymbol{\nu} = \boldsymbol{\Lambda}^{-1}\mathbf{c} + \boldsymbol{\Lambda}^{-1}\boldsymbol{\eta}$.
7.   **If** $\nu_l \in \mathcal{L}$ and $|\nu_l - \lfloor \nu_l \rceil| \le \tau$, for any $3 \le l \le L$
8.   Calculate corresponding LSE ϵ_1 from (46) according to the obtained n_1, n_2, and $\boldsymbol{\nu}$.
9.   **If** $\epsilon_1 < \epsilon$
10. $\epsilon = \epsilon_1$, $(x, y) = (\lfloor \nu_1 \rceil, \lfloor \nu_2 \rceil)$.
11.   **End if**
12.   **End if**
13.   **End**

Further effort to reduce the complexity is illustrated as follows (also applicable for SD approach). From

$$x \sin \theta_i + y \cos \theta_i - n_i = c_i, \tag{50}$$
$$x \sin \theta_j + y \cos \theta_j - n_j = c_j, \tag{51}$$

$\forall i, j$, we know

$$n_j = n_i + c_i - c_j$$
$$- 2\sqrt{x^2 + y^2} \sin\left(\frac{\theta_i - \theta_j}{2}\right) \cos\left(\frac{\theta_i + \theta_j + 2\phi}{2}\right), \tag{52}$$

where $\tan \phi = \frac{y}{x}$. If no priori knowledge of ϕ is available, we may simply consider

$$\left| \cos\left(\frac{\theta_i + \theta_j + 2\phi}{2}\right) \right| \le 1. \tag{53}$$

So the candidate set for n_j, once n_i is specified, should be

$$\mathcal{L}_{ij} \triangleq \left\{ \left\lceil n_i + c_i - c_j - 2d \left| \sin\left(\frac{\theta_i - \theta_j}{2}\right) \right| \right\rceil \le n_j \right.$$
$$\left. \le \left\lfloor n_i + c_i - c_j + 2d \left| \sin\left(\frac{\theta_i - \theta_j}{2}\right) \right| \right\rfloor \right\}. \tag{54}$$

For LS approach, we can try all $n_1 \in \mathcal{L}$ while the corresponding value of n_2 needs only be picked up from $\mathcal{L}_{12} \cap \mathcal{L}$. For SD approach, each of $\{n_l\}_{l=3}^L$ will have its own searching range $\mathcal{K}_l$ calculated from the standard SD algorithm [31]. However, the range of n_l could be further restricted to $\cap_{i=1}^{l-1} \mathcal{L}_{il} \cap \mathcal{K}_l$.

C. Ways to Increase the Reliability of the Algorithms

Although theoretically the PDA occurs with zero probability when $L \ge 3$, we may still encounter spurious solutions in the noisy environment. For example, at low SNR, it is possible that some spurious $\tilde{x}, \tilde{y}, \{\tilde{n}_l\}_{l=1}^L$ yields a smaller LSE than that of the true solutions. We call this phenomenon as *outlier*. The knowledge of the initial radius d also affects the outlier in the way that the larger the d is, the more the candidates of $\mathbf{n}$ will exist and the more possibly the outlier happens. Note that the outlier is an inherent problem in many fields, for example, in the DOA estimation [21], [34]–[36] and the frequency offset estimation [32], [33] etc.

Generally speaking, the occurrence of outlier could be reduced if:

1) the approximate boundary where the UAV lies is more precisely known. Namely, more precise ranges of both the radius $\sqrt{x^2 + y^2}$ and the angle ϕ could be known a priori, by which means the set of valid n_l is reduced.
2) the number of users is enlarged, namely, the number of DOAs L is enlarged. The validity of this suggestion can be seen directly from (28) , where the unknown variables could be over-determined from more equations.
3) the SNR or the number of the samples of the incoming signal is increased.

In fact it is less practical to implement points 2) and 3), especially when the online processing is required. Thus, the first suggestion seems to be the most reasonable way to improve the reliability. Practically, if the formation of the UAV swarm does not change fast, the previous calculated UAV relative position could act as the center of the new circular range. Besides, the GPS may be helpful to get a rough range of the UAVs. The accuracy of general GPS can be accurate to the meter level. Although it does not achieve the accuracy required for calibration, it has been able to greatly reduce the range of positions. Moreover, in UAV swarm, the UAV's position of movement is based on instructions from the fusion center, so it is possible to know the approximate position of each UAV.

One example on how the ranging affect the reliability is provided here. Consider two UAVs with three and five antennas
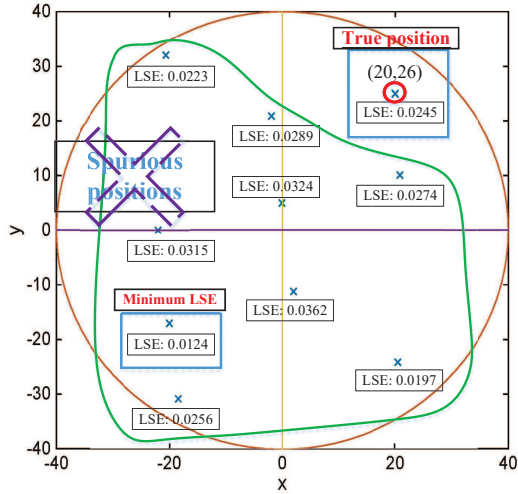
Fig. 2. Detections that correspond to the smallest 10 LSEs.

in the form of uniform linear array (ULA), respectively. The inter-antenna spacing is $\lambda/2$ for each UAV. The unknown displacement of two different UAVs is $(x, y) = (20\lambda, 26\lambda)$, and three different planar signals are from $\theta_1 = -2.5232°$, $\theta_2 = 70.4338°$, and $\theta_3 = 47.1774°$. The SNR is taken as 10 dB and the threshold τ is set as 0.1. The positions of estimated $(\hat{x}, \hat{y})$ that yield the 10 smallest LSE are shown in Fig. 2. The numerical results show that the correct estimation does not give the minimum LSE. Nevertheless, since the positions of estimated $(\hat{x}, \hat{y})$ is so sparse, even a few more information will be very helpful in removing the spurious results. In fact, it is not hard for one to obtain the priori observation that the second UAV stays in the first quadrant. Then, the number of the candidates immediately reduces to 2 among which the correct solution yields the smallest LSE.

Remark 5. *Although the antennas of each UAV is less than the number of users, the proposed algorithm can work as long as the total number of antennas of the UAV swarm is greater than the number of users. Meanwhile, The proposed algorithm is particularly not affected by the randomly joining and exiting UAVs, namely robust.*

D. Cramer-Rao Bound of the Positioning

Assume the observations satisfy the following deterministic model

$$\mathbf{x}(t) \sim \mathcal{N}\{\mathbf{A}(\theta)\mathbf{\Omega}\mathbf{s}(t), \sigma_n^2\mathbf{I}\}, \quad t = 1, 2, \cdots, N. \quad (55)$$

The displacements of different UAVs are represented by the $2(K-1) \times 1$ vector

$$\boldsymbol{\eta} = [\boldsymbol{\xi}_x^T, \boldsymbol{\xi}_y^T]^T, \quad (56)$$

where $\boldsymbol{\xi}_x^T \triangleq [x'_{21}, x'_{31}, \cdots, x'_{K1}]$ and $\boldsymbol{\xi}_y^T \triangleq [y'_{21}, y'_{31}, \cdots, y'_{K1}]$ are treated as unknown parameters along with the source DOAs $\boldsymbol{\theta}$, the deterministic source waveforms $\mathbf{s}(t)$ and the noise variance σ_n^2. We will only derive the $2(K-1) \times 2(K-1)$ $\mathrm{CRB}(\boldsymbol{\eta})$ of the full CRB

matrix. The following theorem presents the closed-form expression for the deterministic CRB.

Theorem 3. *$\mathrm{CRB}(\boldsymbol{\eta})$ is given by*

$$\mathrm{CRB}(\boldsymbol{\eta}) = \frac{\sigma_n^2}{2}(\mathbf{F} - \mathbf{M}\mathbf{Q}^{-1}\mathbf{M}^T)^{-1}, \quad (57)$$

where

$$\mathbf{F} = \sum_{t=1}^{N} \Re\{\mathbf{G}^H(t)\mathbf{\Pi}_\mathbf{A}^\perp \mathbf{G}(t)\},$$

$$\mathbf{M} = \sum_{t=1}^{N} \Re\{\mathbf{G}^H(t)\mathbf{\Pi}_\mathbf{A}^\perp \mathbf{D}(t)\},$$

$$\mathbf{Q} = \sum_{t=1}^{N} \Re\{\mathbf{D}^H(t)\mathbf{\Pi}_\mathbf{A}^\perp \mathbf{D}(t)\},$$

$$\mathbf{\Pi}_\mathbf{A} = \mathbf{A}(\mathbf{A}^H\mathbf{A})^{-1}\mathbf{A}^H,$$

$$\mathbf{\Pi}_\mathbf{A}^\perp = \mathbf{I} - \mathbf{\Pi}_\mathbf{A},$$

$$\mathbf{D}(t) = \left[\frac{\partial\mathbf{a}_1}{\partial\theta_1}\mathbf{s}_1(t), \frac{\partial\mathbf{a}_2}{\partial\theta_2}\mathbf{s}_2(t), \cdots, \frac{\partial\mathbf{a}_L}{\partial\theta_L}\mathbf{s}_L(t)\right],$$

$$\mathbf{G}(t) = [\tilde{\mathbf{G}}(t), \bar{\mathbf{G}}(t)],$$

$$\tilde{\mathbf{G}}(t) = j(2\pi/\lambda)\bar{\mathbf{Y}} \odot (\mathbf{A}\mathbf{\Phi}\mathbf{\Omega}\mathbf{s}(t)\mathbf{1}^T),$$

$$\bar{\mathbf{G}}(t) = j(2\pi/\lambda)\bar{\mathbf{Y}} \odot (\mathbf{A}\mathbf{\Psi}\mathbf{\Omega}\mathbf{s}(t)\mathbf{1}^T),$$

$$\mathbf{\Phi} = \mathrm{diag}\{\sin\theta_1, \sin\theta_2, \cdots, \sin\theta_L\},$$

$$\mathbf{\Psi} = \mathrm{diag}\{\cos\theta_1, \cos\theta_2, \cdots, \cos\theta_L\}. \quad (58)$$

In addition, $\mathbf{1}$ is the $(K-1) \times 1$ vector of ones and the $M \times (K-1)$ matrix $\bar{\mathbf{Y}}$ is obtain by deleting the first column of matrix $\mathbf{V}(\theta)$ and replacing each non-zero entry with 1.

Proof: Let $\boldsymbol{\omega} = [\boldsymbol{\eta}^T, \boldsymbol{\theta}^T]^T$ be the $(2(K-1)+L) \times 1$ vector consisting all the real parameters. From [42], we know

$$\mathrm{CRB}(\boldsymbol{\omega}) = \frac{\sigma_n^2}{2}\begin{bmatrix} \mathbf{F} & \mathbf{M} \\ \mathbf{M}^T & \mathbf{Q} \end{bmatrix}^{-1}. \quad (59)$$

The CRB of $\boldsymbol{\eta}$ is the upper-left block of $\mathrm{CRB}(\boldsymbol{\omega})$. From the partitioned matrix inversion formula [42], $\mathrm{CRB}(\boldsymbol{\eta})$ is calculated as the one in (57). ∎

TABLE I
MAIN SIMULATION PARAMETERS.

Parameter	Description	Value
f_c	Carrier frequency	2.4GHz
λ	Carrier wavelength	0.125m
d_a	Inter-element displacement	0.0625m
τ	Threshold in positioning algorithm	0.2
N	Number of snapshots	200
L	Number of target users	4
d	Maximum radius of UAV swarm	10m

V. SIMULATION RESULTS

In this section, we provide various examples to examine the proposed studies. Three UAVs which have linear subarrays with inter-element displacement $\lambda/2$ are considered. We assume the position of the first antenna in the first UAV is $(x_1, y_1) = (0, 0)$, the position of the first antenna in the second UAV is $(x_2, y_2) = (15\lambda, 50\lambda)$, and the position of the first antenna in the third UAV is $(x_3, y_3) = (30\lambda, 30\lambda)$,
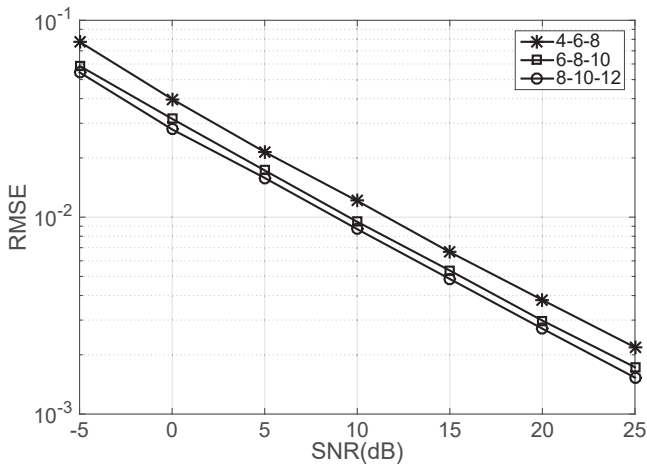
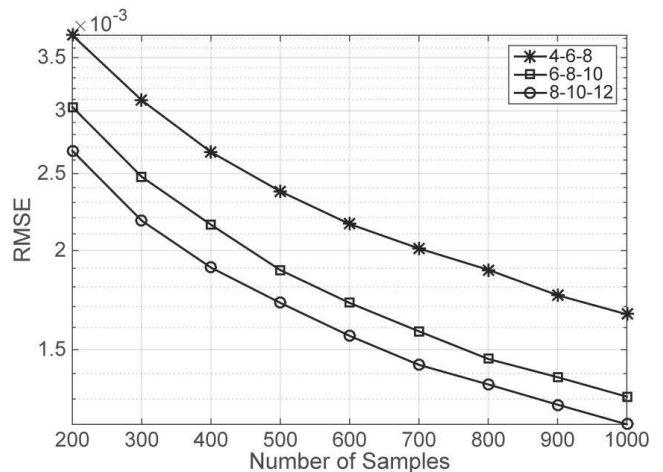Fig. 3. The RMSE performance comparison of $\mathbf{g}(\theta)$, with different number of UAV antennas.

Fig. 4. The RMSE performance comparison of $\mathbf{g}(\theta)$ versus the number of samples, three DOAs case, with different number of UAV antennas.

which is treated as an unknown parameters. The target users are randomly distributed. The number of antennas in each UAV is 12 unless specifically mentioned. The main simulation parameters are given in Table I. The channel vector between the UAV swarm and the target user can be produced according to (1). In all examples, the carrier frequency is assumed as 2.4GHz. We take 200 samples to obtain the covariance matrix unless otherwise mentioned. Since the RMSE performance of the DOA estimation is given in [21], [22], we will not go into details of the DOA estimation here. The figure of the merit is the root-mean-square error (RMSE) defined as

$$\text{RMSE}(\mathbf{g}(\theta)) = \sqrt{\frac{1}{L}\sum_{l=1}^{L}\mathbb{E}\{(\hat{\mathbf{g}}(\theta_l) - \mathbf{g}(\theta_l))^2\}},$$

$$\text{RMSE}(x) = \sqrt{(\mathbb{E}\{(\hat{x}_2(i) - x_2)^2\} + \mathbb{E}\{(\hat{x}_3(i) - x_3)^2\})/2},$$

$$\text{RMSE}(y) = \sqrt{(\mathbb{E}\{(\hat{y}_2(i) - y_2)^2\} + \mathbb{E}\{(\hat{y}_3(i) - y_3)^2\})/2},$$

where $(\hat{x}(i), \hat{y}(i))$ is the estimate of (x, y) in the ith run. When the threshold τ is chosen sufficiently large, e.g., $\tau = 0.2$, the LS and the SD algorithms yield the similar performance so we will only provide the simulation results for LS algorithm.

In the first example, we consider three different type of UAV swarms with three UAVs, and the subarray of the UAVs of different types contains $(4, 6, 8)$, $(6, 8, 10)$, and $(8, 10, 12)$ antennas. We show the RMSE performance of $\mathbf{g}(\theta)$ as a function of SNR in Fig. 3 for three DOAs $\boldsymbol{\theta} = [0°, 30°, 50°]$, where the RMSE is similarly defined as in (60). We see that the RMSEs of all three $\mathbf{g}(\theta)$ linearly decreasing as SNR increases. In addition, increasing the number of UAV antennas will improve the estimation accuracy of $\mathbf{g}(\theta)$. Moreover, $\mathbf{g}(\theta)$ can be correctly estimated with three DOAs.

Fig. 4 shows the RMSE performance of $\mathbf{g}(\theta)$ under different number of the samples at SNR= 20dB for three DOAs $\boldsymbol{\theta} = [0°, 30°, 50°]$. As claimed in Section III, the RARE estimator provides more accurate estimation of both $\boldsymbol{\theta}$ when the number of the samples increases. In turn, the performance of $\mathbf{g}(\theta)$ estimation is also improved. Moreover, it can be seen that estimation accuracy of $\mathbf{g}(\theta)$ will be improved when the
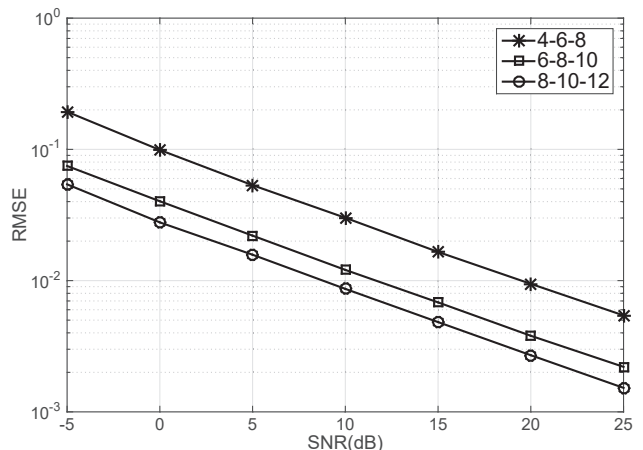

Fig. 5. The RMSE performance comparison of channel estimation, with different number of UAV antennas.

number of UAV antennas increases.

Fig. 5 plots the RMSE performances of channel estimation as a function of SNR for various UAV antenna sizes where the default value of training sequence $p = L = 3$. We assume that the total transmit power for each user are constrained constantly. It is clearly seen from Fig. 5 that increasing the number of UAV antennas improves the channel estimation accuracy due to the improved DOA accuracy and the accuracy of $\mathbf{g}(\theta)$.

In Fig. 6, four signals from $\boldsymbol{\theta} = [-10°, 0°, 30°, 50°]$ impinge on the UAV swarm array. Fig. 6 shows the RMSEs of x and y versus the SNR for $d = 15\lambda$ and $\phi \in [30°, 120°]$ are known a priori. Namely, the antenna is located in a quadrant area. The corresponding CRBs of x and y are also displayed In Fig. 6. For this scenario, the RMSEs of x and y match their corresponding CRBs very well at high SNR region, and the outlier appears until SNR is no less than 5 dB.

We then examine the proposed algorithm under different number of users. Fig. 7 show the RMSE performance of the UAV positioning versus SNR for three DOAs
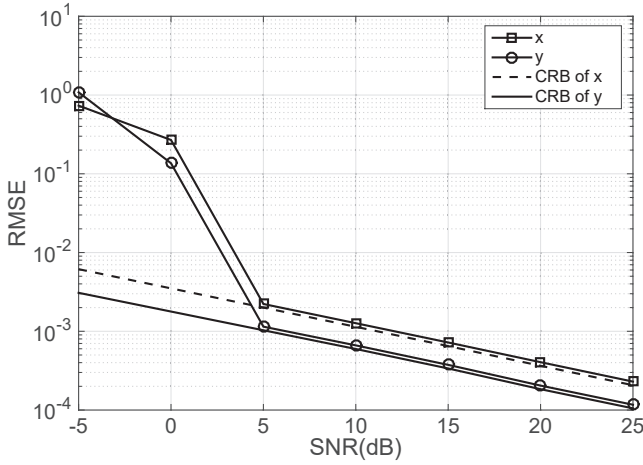
Fig. 6. The RMSE and CRB performance of UAV positioning versus the SNR for four DOAs case with $d = 75\lambda$ and $\phi \in [30°, 120°]$.
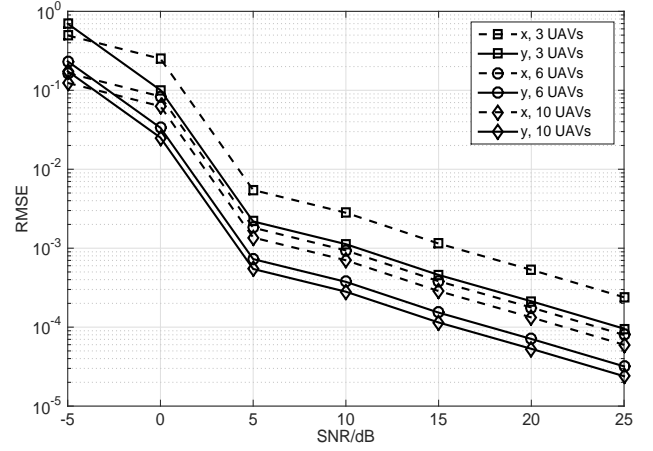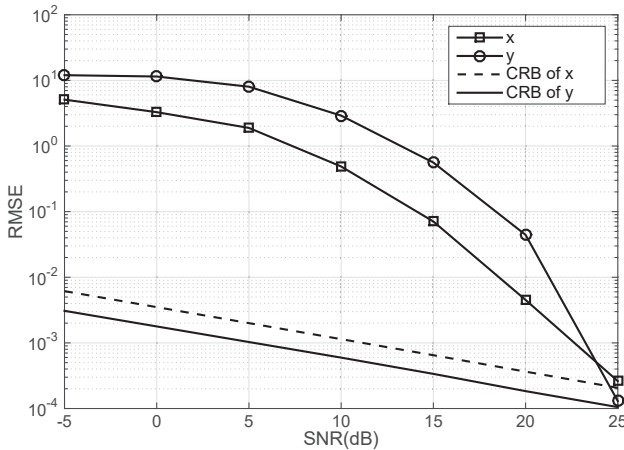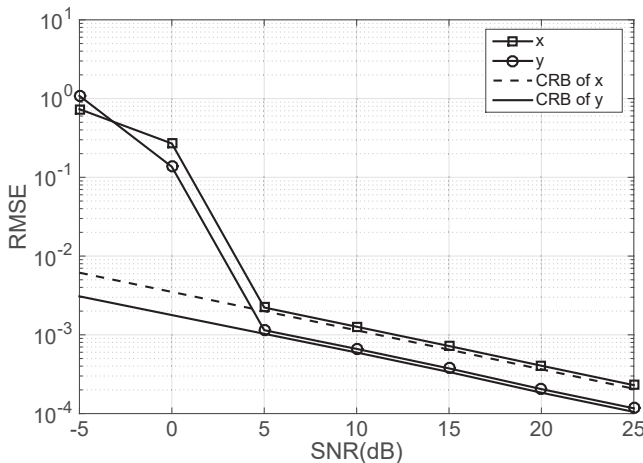

Fig. 8. The RMSE performance of UAV positioning versus the SNR for four DOAs case with different number of UAVs.

(a) Three DOAs

Fig. 9. The RMSE performance of UAV positioning versus the number of samples at SNR = 5 dB.

(b) Five DOAs

Fig. 7. The RMSE and CRB performance of UAV positioning versus the SNR with $d = 75\lambda$ and $\phi \in [30°, 120°]$.

from $\boldsymbol{\theta} = [0°, 30°, 50°]$ and five DOAs from $\boldsymbol{\theta} = [-10°, 0°, 10°, 30°, 50°]$, respectively. We see that in terms of positioning RMSE, five DOAs do not improve much compared

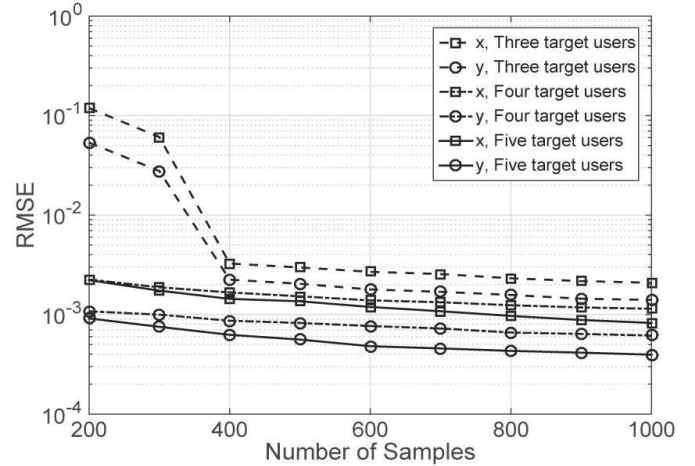to four DOAs. However, using three DOAs meets severe outlier effect. With three DOAs, the estimation under the proposed scenario could not avoid the outlier over low SNR region, and it only gives reliable result after SNR is higher than 25 dB. The reason is that three different DOAs are the theoretical limit on the number of DOAs and may suffer from outlier in the noisy environment.

Fig. 8 plots RMSEs of x and y versus the SNR for different number of UAVs, where each UAV has 4 antennas. Four signals from $\boldsymbol{\theta} = [-10°, 0°, 30°, 50°]$ impinge on the UAV swarm array. It can be seen from Fig. 8 that the outlier disappears when SNR is no less than 5 dB, and the proposed positioning algorithm provides more accurate estimation of both x, y when the number of the UAVs increases.

To gain more insight on the effect of the number of DOAs, we display RMSE performance of x and y under different number of the samples at SNR= 5dB for three DOAs, four DOAs, and five DOAs in Fig. 9. It is shown that increasing DOAs will improve the performance in terms of RMSE efficiently, especially in the small number of samples,
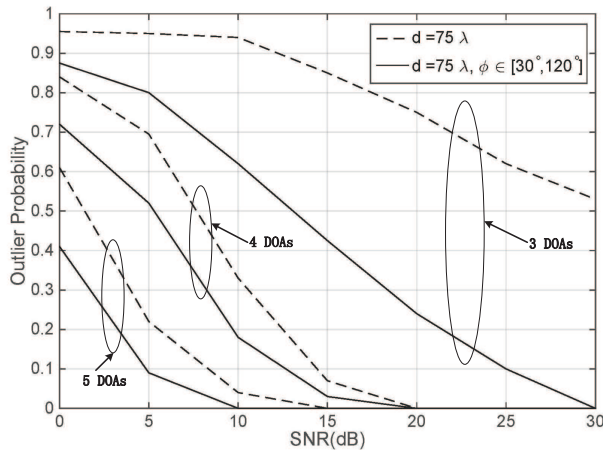
Fig. 10. Outlier probability versus the SNR with three DOAs, four DOAs and five DOAs.

Fig. 11. Sum rate comparison of different number of UAVs are displayed for comparison as a function of SNR.

Moreover, it is also seen that using five DOAs will not improve the performances in terms of RMSEs very much than using four DOAs.

TABLE II
DETECTION OF THE UAV POSITIONS.

SNR = 0 dB				
x	-8.4375	-37.7320	-40.7365	51.3175	15.4024
y	0.1170	-34.3500	30.3885	-0.3020	50.9752
ϵ	0.0245	0.0305	0.0360	0.0409	0.0436
option	spurious	spurious	spurious	spurious	true
SNR = 10 dB				
x	45.3776	15.0048	-40.0619	-5.6891	20.6836
y	15.9859	-49.9908	30.0235	0.5186	-25.9863
ϵ	0.0146	0.0182	0.0241	0.0273	0.0306
option	spurious	true	spurious	spurious	spurious
SNR = 20 dB				
x	15.0010	45.3539	-5.6894	-40.0423	50.2711
y	49.9977	20.0029	0.0769	30.0117	-40.0196
ϵ	0.0055	0.0161	0.0275	0.0310	0.0491
option	true	spurious	spurious	spurious	spurious

It is then of interest to check the effect of different SNR on spurious estimation results. Here we only consider two UAVs where the position of the first antenna in the second UAV is $(x_2, y_2) = (15\lambda, 50\lambda)$. The radius $d = 75\lambda$ is known a priori. We record five detection results that yield five smallest LSEs in Table II. The SNR values are taken as 0 dB, 10 dB, and 20 dB, respectively. It can be seen that the true solution ranks 5th according to LSE at SNR= 0 dB. However, when SNR increases to 10 dB, only one spurious detection gives smaller LSE than the true solution. In fact, this spurious detection could be removed if the priori knowledge of the angle ϕ is known. Nevertheless, when SNR goes to 20 dB, the true solution gives the smallest LSE even when we only know the radius d.

To gain more insight on the effect of the number of DOAs, we display the outlier probabilities for three DOAs, four DOAs and five DOAs in Fig. 10. We can see that when only the radius d is known as priori, the corresponding outlier probability of five DOAs is much less than that of the four DOA case. Moreover, using three DOAs still has the potential to avoid
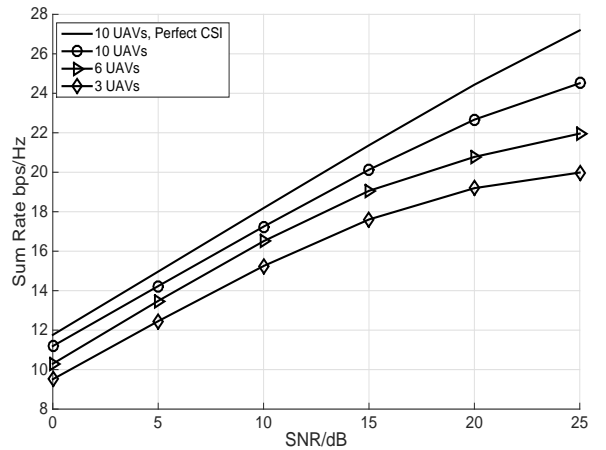
the outlier when SNR is sufficiently high.

Fig. 11 plots the achievable sum rate for the downlink data transmission with different number of UAVs in the UAV swarm, where each UAV has 4 antennas. To make the comparison fair, the overall data power are set as the same for all methods. It can be seen from Fig. 11 that with the increasing of the number of UAVs, the performances become better and are even comparable to the performance of the prefect CSI case, in any SNR values.

VI. CONCLUSION

In this paper, we proposed a new channel estimation and self-positioning method for the UAV swarm under the practical consideration that each UAV has a well calibrated array and the UAVs are displaced by arbitrarily unknown displacement due to the dynamic moving. We adopted RARE algorithm to obtain the DOA information of target user blindly. Then the channel gain estimation was performed with very small amount of training resources. Next we developed two efficient algorithms for the positioning estimation that avoid the exhaustive searching over the entire lattice region. Meanwhile, several ways to improve the detection accuracy were suggested. Moreover, the deterministic CRB of the self-positioning estimation was derived in close-form. It was shown that our proposed channel estimation and self-positioning method have satisfactory performance, especially when the number of the existing signals increases, the SNR arises, and the number of the samples increases.

VII. APPENDIX
DERIVATION OF THE PROJECTION MATRIX

Denote the first and the second columns of $\mathbf{G}$ as

$$\mathbf{v}_1 = [\sin\theta_1, \sin\theta_2, \cdots, \sin\theta_L]^T, \tag{60}$$
$$\mathbf{v}_2 = [\cos\theta_1, \cos\theta_2, \cdots, \cos\theta_L]^T, \tag{61}$$

respectively. Then $(\mathbf{G}^T\mathbf{G})^{-1}$ can be calculated as

$$
\begin{aligned}
(\mathbf{G}^T\mathbf{G})^{-1} &= \left(\left[\begin{array}{c} \mathbf{v}_1^T \\ \mathbf{v}_2^T \end{array} \right] \left[\begin{array}{cc} \mathbf{v}_1 & \mathbf{v}_2 \end{array} \right] \right)^{-1} \\
&= \left[\begin{array}{cc} \sum_i \sin^2\theta_i & \sum_i \sin\theta_i\cos\theta_i \\ \sum_i \sin\theta_i\cos\theta_i & \sum_i \cos^2\theta_i \end{array} \right]^{-1} \\
&= \frac{1}{D} \left[\begin{array}{cc} \sum_i \cos^2\theta_i & -\sum_i \sin\theta_i\cos\theta_i \\ -\sum_i \sin\theta_i\cos\theta_i & \sum_i \sin^2\theta_i \end{array} \right] \\
&= \frac{1}{D} \left[\begin{array}{c} -\mathbf{v}_2^T \\ \mathbf{v}_1^T \end{array} \right] \left[\begin{array}{cc} -\mathbf{v}_2 & \mathbf{v}_1 \end{array} \right],
\end{aligned} \tag{62}
$$

where

$$
\begin{aligned}
D &= \det\{\mathbf{G}^T\mathbf{G}\} \\
&= \sum_i \sum_j \sin^2\theta_i\cos^2\theta_j - \sum_i \sum_j \sin\theta_i\cos\theta_i\sin\theta_j\cos\theta_j \\
&= \sum_i \sum_{j\neq i} \sin^2\theta_i\cos^2\theta_j - 2\sum_i \sum_{j>i} \sin\theta_i\cos\theta_i\sin\theta_j\cos\theta_j \\
&= \sum_i \sum_{j>i} \sin^2(\theta_i - \theta_j).
\end{aligned} \tag{63}
$$

Then the projection matrix $\mathbf{P}_{\boldsymbol{\theta}}$ is given by

$$
\begin{aligned}
\mathbf{P}_{\boldsymbol{\theta}} &= \mathbf{G}(\mathbf{G}^T\mathbf{G})^{-1}\mathbf{G}^T \\
&= \frac{1}{D} \left[\begin{array}{cc} \mathbf{v}_1 & \mathbf{v}_2 \end{array} \right] \left[\begin{array}{c} -\mathbf{v}_2^T \\ \mathbf{v}_1^T \end{array} \right] \left[\begin{array}{cc} -\mathbf{v}_2 & \mathbf{v}_1 \end{array} \right] \left[\begin{array}{c} \mathbf{v}_1^T \\ \mathbf{u}_2^T \end{array} \right] \\
&= \frac{1}{D} \mathbf{B}\mathbf{B}^T,
\end{aligned} \tag{64}
$$

where

$$
\mathbf{B} = \mathbf{v}_2\mathbf{v}_1^T - \mathbf{v}_1\mathbf{u}_2^T, \tag{65}
$$

whose (i,j)th entry is given by

$$
[\mathbf{B}]_{ij} = \cos\theta_i\sin\theta_j - \sin\theta_i\cos\theta_j = \sin(\theta_j - \theta_i). \tag{66}
$$

REFERENCES

[1] Y. Zeng, R. Zhang, and T. J. Lim, "Wireless communications with unmanned aerial vehicles: opportunities and challenges," *IEEE Commun. Mag.*, vol. 54, no. 5, pp. 36–42, May 2016.

[2] L. Gupta, R. Jain and G. Vaszkun, "Survey of important issues in UAV communication networks," *IEEE Commun. Surveys Tuts.*, vol. 18, no. 2, pp. 1123–1152, Second quarter 2016.

[3] H. Kim and Y. Kim, "Trajectory optimization for unmanned aerial vehicle formation reconfiguration," *Engineering Optimization*, vol. 46, no. 1, pp. 84–106, Jan. 2014.

[4] M. Tortonesi, C. Stefanelli, E. Benvegnu, K. Ford, N. Suri and M. Linderman, "Multiple-UAV coordination and communications in tactical edge networks," *IEEE Commun. Mag.*, vol. 50, no. 10, pp. 48–55, Oct. 2012.

[5] L. Gupta, R. Jain, and G. Vaszkun, "Survey of important issues in UAV communication networks," *IEEE Commun. Surveys and Tutorials*, vol. 18, no. 2, pp. 1123–1152, Nov. 2015.

[6] H. Jiang, Z. C. Zhang, and G. Gui, "Three-dimensional non-stationary wideband geometry-based UAV channel model for A2G communication environments", *IEEE Access.* vol. 7, pp. 26116–26122, Mar. 2019.

[7] Z. Xiao, P. Xia, and X. Xia, "Enabling UAV cellular with millimeter wave communication: potentials and approaches," *IEEE Commun. Mag.*, vol. 54, no. 5, pp. 66–73, May 2016.

[8] T. S. Rappaport, E. Ben-Dor, J. N. Murdock, and Y. Qiao, "38 GHz and 60 GHz angle-dependent propagation for cellular peer-to-peer wireless communications," in *Proc. of IEEE ICC12*, pp. 4568–4573, Jun. 2012.

[9] Z. Pi and F. Khan, "An introduction to millimeter-Wave mobile broadband systems, *IEEE Commun. Mag.*, vol. 49, no. 6, pp. 101–107, Jun. 2011.

[10] M. L. Bhavsar, R. Sharma, and A. Bhattacharya, "Monolithic Ka to Ku-band all balanced sub-harmonic resistive MHEMT mixer for satellite transponder," *IEEE Microw. Compon. Lett.*, vol. 25, no. 5, pp. 316–318, Apr. 2015.

[11] W. Liu and D. G. Michelson, "Effect of turbulence layer height and satellite altitude on tropospheric scintillation on Ka-band earth-LEO satellite links," *IEEE Trans. Veh. Technol.*, vol. 59, no. 7, pp. 3182–3192, Sep. 2010.

[12] F. Rusek, "Scaling up MIMO: opportunities and challenges with very large arrays," *IEEE Signal Process. Mag.*, vol. 30, no. 1, pp. 40–60, Jan. 2013.

[13] T. L. Marzetta, "Noncooperative cellular wireless with unlimited numbers of base station antennas," *IEEE Trans. Wireless Commun.*, vol. 9, no. 11, pp. 3590–3600, Nov. 2010.

[14] F. Boccardi, R. W. Heath, A. Lozano, T. L. Marzetta, and P. Popovski, "Five disruptive technology directions for 5G," *IEEE Commun. Mag.*, vol. 52, no. 2, pp. 74–80, Feb. 2014.

[15] H. Xie, B. Wang, F. Gao, and S. Jin, "A full-space spectrum-sharing strategy for massive MIMO cognitive radio," *IEEE J. Select. Areas Commun.*, vol. 34, no. 10, pp. 2537–2549, Oct. 2016.

[16] H. Xie, F. Gao, and S. Jin, "An overview of low-rank channel estimation for massive MIMO systems," *IEEE Access*, vol. 4, pp. 7313–7321, Nov. 2016.

[17] R. W. Heath, N. G. Prelcic, S. Rangan, W. Roh, and A. Sayeed, "An overview of signal processing techniques for millimeter wave MIMO systems," *IEEE J. Sel. Topic Signal Process.*, vol. 10, no. 3, pp. 436–453, Apr. 2016.

[18] H. Xie, F. Gao, S. Zhang, and S. Jin, "Spatial-temporal BEM and channel estimation strategy for massive MIMO time-varying systems," in *Proc. of IEEE GLOBECOM16*, Washington DC, USA, pp. 1–6, Dec. 2016.

[19] B. Parkinson and J. Spilker, *Global Positioning System: Theory and Application*. American Institute of Astronautics and Aeronautics, 1996.

[20] N. M. Drawil, H. M. Amar, and O. A. Basir, "GPS localization accuracy classification: A context-based approach", *IEEE Trans. Intelligent Transportation Systems*, vol. 14, no. 1, pp. 262–273, Mar. 2013.

[21] M. Pesavento, A. B. Gershman, and K. M. Wong, "Direction finding in partly-calibrated sensor arrays composed of multiple subarrays," *IEEE Trans. Signal Proscessing*, vol. 50, no. 9, pp. 2103–2115, Sep. 2002.

[22] C. M. S. See and A. B. Gershman, "Direction-of-arrival estimation in partly calibrated subarray-based sensor arrays," *IEEE Trans. Signal Processing*, vol. 52, no. 2, pp. 329–338, Feb. 2004.

[23] J. T.-H. Lo and S. L. Marple Jr., "Eigenstructure methods for array sensor localization," in *Proc. ICASSP87*, Dallas, USA, vol. 4, Apr. 1987, pp. 2260–2263.

[24] J. Sheinvald, M. Wax, and A. J. Weiss, "Localization of multiple sources with moving arrays," *IEEE Trans. Signal Processing*, vol. 46, no. 10, pp. 2736–2743, Oct. 1998.

[25] J. Zhao, F. Gao, Q. Wu, S. Jin, Y. Wu, and W. Jia, "Beam Tracking for UAV Mounted SatCom on-the-Move with Massive Antenna Array," *IEEE J. Select. Areas Commun.*, vol. 36, no. 2, pp. 363–375, Feb. 2018.

[26] F. Gao, R. Zhang, and Y.-C. Liang, "Channel estimation for OFDM modulated two-way relay networks," *IEEE Trans. Signal Process.*, vol. 57, no. 11, pp. 4443–4455, Nov. 2009.

[27] H. Xie, F. Gao, S. Zhang, and S. Jin, "An unified transmission strategy for TDD/FDD massive MIMO systems with spatial basis expansion model," *IEEE Trans. Veh. Technol.*, vol. 66, no. 4, pp. 3170–3184, April 2016.

[28] D. Fan, F. Gao, G. Wang, Z. Zhong, and A. Nallanathan, "Angle Domain Signal Processing aided Channel Estimation for Indoor 60GHz TDD/FDD Massive MIMO Systems," *IEEE J. Sel. Areas Commun.* vol. 35, no. 9, pp. 1948–1961, Jun. 2017.

[29] B. Hassibi and H. Vikalo, "On the sphere decoding algorithm I: expected complexity," *IEEE Trans. Signal Processing*, vol. 53, no. 8, pp. 2806–2818, Aug. 2005.

[30] H. Vikalo and B. Hassibi, "On the sphere-decoding algorithm II: generalizations, second-Order statistics, and applications to communications," *IEEE Trans. Signal Processing*, vol. 53, no. 8, pp. 2819–2834, Aug. 2005.

[31] M. O. Damen, K. Abed-Meraim, and J.-C. Belfiore, "Generalised sphere decoder for asymmetrical space-time communication architecture," *IEEE Elect. Lett.*, vol. 36, pp. 166–167, Jan. 2000.

[32] F. Gao and A. Nallanathan, "Blind maximum likelihood CFO estimation for OFDM systems via polynomial rooting", *IEEE Signal Processing Lett.*, vol. 13, no. 2, pp. 73–76, Feb. 2006.

[33] F. Gao, T. Cui, and A. Nallanathan, "Scattered pilots and virtual carriers based frequency offset tracking for OFDM systems: algorithms,

identifiability, and performance analysis", *IEEE Trans. Commun.*, vol. 56, no. 4, pp. 619–629, Apr. 2008.

[34] R. Schmidt, "Multiple emitter location and signal parameter estimation," *IEEE Trans on Antennas Propag.*, vol. 34, no. 3, pp. 276–280, Mar. 1986.

[35] R. Roy, and T. Kailath, "ESPRIT-Estimation of signal parameters via rotational invariance techniques," *IEEE Trans. Acoust., Speech, Signal Processing*, vol. 37, pp. 984–995, July 1989.

[36] B. Friedlander, "A sensitivity analysis of the MUSIC algorithm," *IEEE Trans. Acoust., Speech, Signal Processing*, vol. 38, pp. 1740–1751. Oct. 1990.

[37] B. Porat, and B. Friedlander, "Accuracy requirements in off-line array calibra- tion," *IEEE Trans. Aerosp. Electron. Syst.*, vol. 33, pp. 545–556, Apr. 1997.

[38] V. J. Bowman, and C.-A. Burdet, "On the general solution to systems of mixed-integer linear equations," *SIAM J. Appl. Math.*, vol. 26, no. 1, pp. 120–125, Jan. 1974.

[39] H. J. S. Smith, "On systems of linear indeterminate equations and congruences," *Trans. Philos.*, vol. 151, pp. 293–326, 1861.

[40] M. F. Hurt, and C. Waid, "A generalized inverse which gives all the integral solutions to a system of linear equations," *SIAM J. Appl. Math.*, vol. 19, no. 3, pp. 547–550, Nov. 1970.

[41] M. Tawarmalani and N. V. Sahinidis, Convexification and Global Optimization in Continuous and Mixed-Integer Nonlinear Programming: Theory, Algorithms, Software, and Applications, Nonconvex Optimization and Its Applications Series. Kluwer Academic Publishers, Boston MA, 2003.

[42] P. Stoica and R. Moses, *Introduction to Spectral Analysis*. Upper Saddle River, NJ: Prentice-Hall 1997.

Dian Fan received the B.Eng. degree from the School of Science, Beijing Jiaotong University (BJTU), Beijing, China, in 2014, and the Ph.D. degree from the School of Science, Beijing Jiaotong University (BJTU), Beijing, China, in 2019. He is currently working in the China Academy of Information and Communications Technology, Beijing, China. He was a Visiting Ph.D. Student at the Department of Informatics at King's College London from October 2016 to March 2017, and at the School of Electronic Engineering and Computer Science at Queen Mary University of London from October 2017 to September 2018. His research interests include MIMO techniques, massive MIMO systems, millimeter wave systems and array signal processing.

Feifei Gao (M'09, SM'14) received the B.Eng. degree from Xian Jiaotong University, Xi'an, China in 2002, the M.Sc. degree from McMaster University, Hamilton, ON, Canada in 2004, and the Ph.D. degree from National University of Singapore, Singapore in 2007. He was a Research Fellow with the Institute for Infocomm Research (I2R), A*STAR, Singapore in 2008 and an Assistant Professor with the School of Engineering and Science, Jacobs University, Bremen, Germany from 2009 to 2010. In 2011, he joined the Department of Automation, Tsinghua University, Beijing, China, where he is currently an Associate Professor.

Prof. Gao's research areas include communication theory, signal processing for communications, array signal processing, and convex optimizations, with particular interests in MIMO techniques, multi-carrier communications, cooperative communication, and cognitive radio networks. He has authored/coauthored more than 120 refereed IEEE journal papers and more than 120 IEEE conference proceeding papers.

Prof. Gao has served as an Editor of IEEE Transactions on Wireless Communications, IEEE Signal Processing Letters, IEEE Communications Letters, IEEE Wireless Communications Letters, International Journal on Antennas and Propagations, and China Communications. He has also serves as the symposium co-chair for 2018 IEEE Vehicular Technology Conference Spring (VTC), 2015 IEEE Conference on Communications (ICC), 2014 IEEE Global Communications Conference (GLOBECOM), 2014 IEEE Vehicular Technology Conference Fall (VTC), as well as Technical Committee Members for many other IEEE conferences.

Bo Ai received his M.S. degree and Ph.D. degree from Xidian University in China. He graduated from Tsinghua University with the honor of Excellent Postdoctoral Research Fellow at Tsinghua University in 2007. He was a visiting professor at EE Department, Stanford University in 2015. He is now working at Beijing Jiaotong University as a full professor and Ph.D. candidate advisor. He is the Deputy Director of State Key Lab of Rail Traffic Control and Safety, and the Deputy Director of International Joint Research Center. He is one of the main responsible people for Beijing "Urban rail operation control system" International Science and Technology Cooperation Base, and the backbone member of the Innovative Engineering Based jointly granted by Chinese Ministry of Education and the State Administration of Foreign Experts Affairs.

He has authored/co-authored 8 books and published over 300 academic research papers in his research area. He has hold 26 invention patents. He has been the research team leader for 26 national projects and has won some important scientific research prizes. He has been notified by Council of Canadian Academies (CCA) that, based on Scopus database, Prof. Bo Ai has been listed as one of the Top 1% authors in his field all over the world. Prof. Bo Ai has also been Feature Interviewed by IET Electronics Letters. His interests include the research and applications of channel measurement and channel modeling, dedicated mobile communications for rail traffic systems.

Prof. Bo Ai is a Fellow of the Institution of Engineering and Technology (IET Fellow), IEEE VTS Distinguished Lecturer. He is an IEEE VTS Beijing Chapter Vice Chair. IEEE BTS Xi'an Chapter Chair. He was as a Co-chair or a Session/Track Chair for many international conferences. He is an Editor of IEEE Transactions on Consumer Electronics and an Editorial Committee Member of the Wireless Personal Communications journal. He is the Lead Guest Editor for Special Issues on IEEE Transactions on Vehicular Technology, IEEE Antennas and Propagations Letters, International Journal on Antennas and Propagations. He has received many awards such as Outstanding Youth Foundation from National Natural Science Foundation of China, the Qiushi Outstanding Youth Award by Hong Kong Qiushi Foundation, the New Century Talents by the Chinese Ministry of Education, the Zhan Tianyou Railway Science and Technology Award by the Chinese Ministry of Railways, and the Science and Technology New Star by the Beijing Municipal Science and Technology Commission.

Gongpu Wang received the B.Eng. degree in communication engineering from Anhui University, Hefei, Anhui, China, in 2001, and the M.Sc. degree from Beijing University of Posts and Telecommunications, Beijing, China, in 2004. From 2004 to 2007, he was an assistant professor in School of Network Education, Beijing University of Posts and Telecommunications. He received Ph.D. degree from University of Alberta, Edmonton, Canada, in 2011. Currently, he is a full professor in School of Computer and Information Technology, Beijing Jiaotong University, China. His research interests include wireless communication, signal processing, artificial intelligence, and Internet of Things.

Zhangdui Zhong received the B.E. and M.S. degrees from Beijing Jiaotong University, Beijing, China, in 1983 and 1988, respectively. He is currently a Professor and an advisor of Ph.D. candidates with Beijing Jiaotong University, Beijing, China, where he is also a Chief Scientist of the State Key Laboratory of Rail Traffic Control and Safety. He is also a Director of the Innovative Research Team of the Ministry of Education, Beijing, and a Chief Scientist of the Ministry of Railways, Beijing. His interests include wireless communications for railways, control theory and techniques for railways, and GSM-R systems. His research has been widely used in railway engineering, such as at the Qinghai-Xizang railway, the Datong-Qinhuangdao Heavy Haul railway, and many high-speed railway lines in China. He is an Executive Council member of the Radio Association of China, Beijing, and a Deputy Director of Radio Association, Beijing. He has authored or co-authored seven books, five invention patents, and over 200 scientific research papers in his research area. He received the MaoYiSheng Scientific Award of China, the ZhanTianYou Railway Honorary Award of China, and the Top 10 Science/Technology Achievements Award of Chinese Universities.

14

Yansha Deng (S'13-M'18) received the Ph.D. degree in electrical engineering from the Queen Mary University of London, U.K., in 2015. From 2015 to 2017, she was a Post-Doctoral Research Fellow with Kings College London, U.K., where she is currently a Lecturer (Assistant Professor) with the Department of Informatics. Her research interests include molecular communication, Internet of Things, and 5G wireless networks. She was a recipient of the Best Paper Awards from ICC 2016 and Globecom 2017 as the first author. She is currently an Editor of the IEEE TRANSACTIONS ON COMMUNICATIONS and the IEEE COMMUNICATION LETTERS. She also received an Exemplary Reviewer of the IEEE TRANSACTIONS ON COMMUNICATIONS in 2016 and 2017. She has also served as a TPC Member for many IEEE conferences, such as IEEE GLOBECOM and ICC.

Arumugam Nallanathan (S'97-M'00-SM'05-F'17) is Professor of Wireless Communications and Head of the Communication Systems Research (CSR) group in the School of Electronic Engineering and Computer Science at Queen Mary University of London since September 2017. He was with the Department of Informatics at Kings College London from December 2007 to August 2017, where he was Professor of Wireless Communications from April 2013 to August 2017 and a Visiting Professor from September 2017. He was an Assistant Professor in the Department of Electrical and Computer Engineering, National University of Singapore from August 2000 to December 2007. His research interests include 5G Wireless Networks, Internet of Things (IoT) and Molecular Communications. He published nearly 400 technical papers in scientific journals and international conferences. He is a co-recipient of the Best Paper Awards presented at the IEEE International Conference on Communications 2016 (ICC'2016) , IEEE Global Communications Conference 2017 (GLOBE-COM'2017) and IEEE Vehicular Technology Conference 2018 (VTC'2018). He is an IEEE Distinguished Lecturer. He has been selected as a Web of Science Highly Cited Researcher in 2016.

He is an Editor for IEEE Transactions on Communications. He was an Editor for IEEE Transactions on Wireless Communications (2006-2011), IEEE Transactions on Vehicular Technology (2006-2017), IEEE Wireless Communications Letters and IEEE Signal Processing Letters. He served as the Chair for the Signal Processing and Communication Electronics Technical Committee of IEEE Communications Society and Technical Program Chair and member of Technical Program Committees in numerous IEEE conferences. He received the IEEE Communications Society SPCE outstanding service award 2012 and IEEE Communications Society RCC outstanding service award 2014.